



High-resolution multi-parameter monitoring of microbial water quality and particles at two alpine karst springs as a basis for an early-warning system

Simon Frank¹ · Nikolai Fahrmeier¹ · Nadine Goeppert¹  · Nico Goldscheider¹

Received: 25 January 2022 / Accepted: 6 October 2022
© The Author(s) 2022

Abstract

Karst aquifers are important resources for drinking water supply and are very vulnerable to contamination. Microbial concentrations at karst springs, in particular, often vary quickly over a short period of time. In this study, the response of microbial water quality and particle-size distribution of two alpine karst springs to rainfall events was investigated to test and validate parameters that can be used as early-warning systems for fecal contamination. At both investigated karst springs, total organic carbon, particle-size distribution (especially small particle fractions), and particle load show a good correlation to the fecal indicator bacteria *E. coli* and can therefore be used as a real-time indicator of fecal contamination at the investigated springs. In addition to conventional bacterial determination methods, the β -D-glucuronidase activity, which can be measured in near real-time, was used as a novel indicator parameter for fecal contamination. At the event scale, the β -D-glucuronidase (GLUC) activity shows a good correlation to *E. coli* and can be used as an additional real-time indicator of fecal contamination. For the studied springs, when they show two peaks in turbidity and small particles, these two parameters are suitable for an early warning system because the bacterial contamination occurs during the secondary peak of these parameters. These results highlight the vulnerability of karst aquifers and demonstrate the applicability of advanced measurement techniques in detecting fecal contamination in real-time, which is especially important given the time-consuming nature of conventional bacterial detection methods.

Keywords Karst · Groundwater monitoring · Micro-organisms · water quality · particle-size distribution · early warning system · fecal contamination · indicator parameter

Introduction

Karst aquifers are an important source for drinking water supply. Approximately 750 million people worldwide depend on drinking water from these aquifers (Stevanović 2019). In many alpine and Mediterranean countries, karst aquifers contribute substantially to the freshwater supply. Large cities like Rome (Italy), Damascus (Syria), Beirut (Lebanon), and Vienna (Austria) obtain their drinking water from karst aquifers (Kralik 2001; Kresic and Stevanovic 2010). With the worldwide increasing water demand, high

alpine karst aquifers offer a potential untapped for future water supply.

Because recharge to karst aquifers occurs either directly through solutionally enlarged conduits and fractures or through diffuse pathways, these aquifer types often have complex hydrological characteristics (Bakalowicz 2005). Turbulent flow regimes in conduit systems and short residence times lead to a rapid hydraulic and hydrochemical response to rainfall events which results in high vulnerability of karst groundwater (Ford and Williams 2007; Pronk et al. 2007; White 1988).

Fecal pollution of spring waters is typically determined via fecal indicator bacteria (FIB) such as *E. coli* (e.g. Ferguson et al. 2012). In karst aquifers, the microbial water quality often varies quickly over a wide range with short-term peaks in pathogen concentrations. Therefore, the need for rapid assessment and near real-time quantification of FIB is apparent (e.g. Fiksdal and Tryland 2008; World Health

✉ Nadine Goeppert
nadine.goeppert@kit.edu

¹ Institute of Applied Geosciences, Division of Hydrogeology, Karlsruhe Institute of Technology (KIT), Kaiserstr. 12, 76131 Karlsruhe, Germany

Organization 2017). However, standard cultivation-based methods for the detection and enumeration of *E. coli* require between 18 and 72 hours, depending on the incubation time (Wildeboer et al. 2010), a time frame where many individuals are possibly already exposed to pathogens.

Some studies of freshwaters have used organic matter fluorescence as a tracer of groundwater flow in aquifers and especially protein-like fluorescence as a possible indicator of bacterial contamination (Baker and Inverarity 2004; Baker and Lamont-Black 2001). The data of Determann et al. (1998) and Quiers et al. (2014) show tryptophan-like fluorescence to be directly related to the microbial activity of bacteria. Other studies also support the relation between bacteria and tryptophan-like fluorescence and promote the use of peak T fluorescence as a real-time indicator of bacterial contamination (Fellman et al. 2009; Sorensen et al. 2018; Sorensen et al. 2015). However, peak T fluorescence is only a good indicator of bacterial contamination at high contamination levels. At low contamination levels, the correlation between protein-like fluorescence and *E. coli* is not as good as at high contamination levels (e.g. Frank et al. 2018).

Another promising alternative to conventional culture-based bacterial determination methods is enzyme assays because they are relatively easy to perform and can provide results in less than one hour (Fiksdal and Tryland 2008; Heery et al. 2016). About 97 % of *E. coli* strains demonstrate β -D-glucuronidase (GLUC) activity while this enzyme is absent in almost all other coliform bacteria (Wildeboer et al. 2010). GLUC activity is therefore considered as a suitable indicator of *E. coli* bacteria (Farnleitner et al. 2002; Wildeboer et al. 2010). There is increasing research interest in determining GLUC activity in order to evaluate the microbial water quality including development of automated devices for long-term, on-site measurement, such as the ColiMinder (VWMS, Austria). This instrument was tested by Stadler et al. (2016) in an open-air hydrological laboratory. A major outcome of this study was that GLUC activity was not a useful proxy for *E. coli* but further field experiments were required in other outdoor settings. Here, a mobile ColiMinder device was tested at a karst spring in the Austrian Alps to determine the microbial contamination patterns after rain events.

In addition to natural fluorescence and enzymatic activity, turbidity and particle-size distribution were investigated at the two karst springs. Abia et al. (2016) postulated that the risk of an infection due to *E. coli* increases 10-fold if there is a turbidity event because bacteria tend to adhere to particles and are then more persistent within the aquatic environment than free floating bacteria (Dussart-Baptista et al. 2003; Pronk et al. 2006). In karst systems, particles can be transported over large distances and are influenced by processes of sedimentation and mobilization (Mahler et al. 2000). Turbidity itself is a bulk parameter without

any information about the origin or nature of the detected particles. The measurement of the particle-size distribution (PSD) can deliver more information and is a valuable tool to specify the type of turbidity and to identify particle-size classes that are possibly related to bacterial contamination (Ender et al. 2017; Frank et al. 2018; Pronk et al. 2007).

This study aims to determine parameters that can be used as early-warning parameters or at least real-time indicators of fecal contamination at karst springs. In this study, a mobile ColiMinder device was tested and compared the results to conventional bacterial determination methods and fluorescence measurements. Furthermore, turbidity and particle-size distribution are compared to bacterial and enzymatic measurements and evaluated as complementary parameters to assess their suitability as parameters for early- or real-time warning parameters.

The main research questions of this study are:

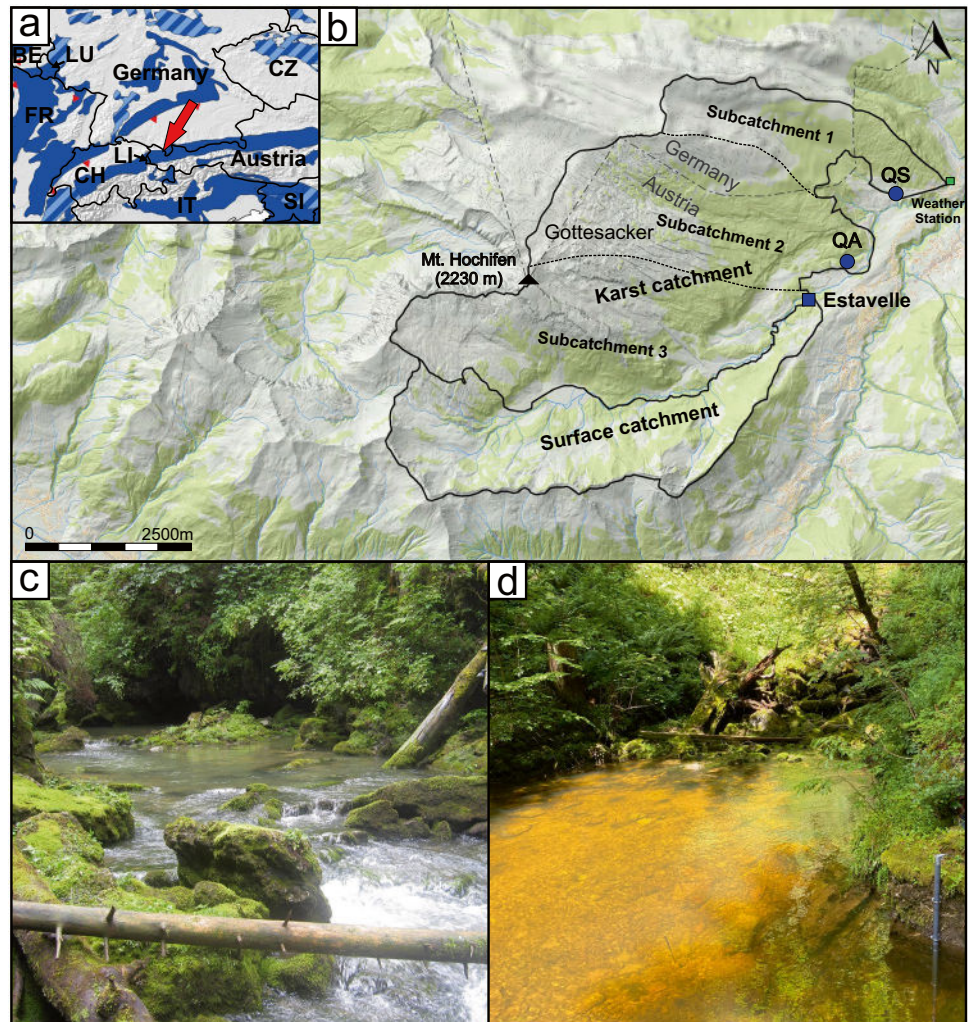
- How does the measured enzymatic activity (GLUC) react to a rainfall event compared to turbidity and particle-size distribution?
- What is the relation between GLUC activity and conventional cultivation-based determination methods of *E. coli* as well as to other water quality parameters?
- What information about the investigated karst system can be obtained from the measured parameters?
- Is one of the investigated parameters, or a combination of several parameters, suitable for the use of an early-warning or real-time indication system for bacterial contamination?

Study site and methods

Study site

The study area is located along the eastern flank of Mount Hochifen in the northern Alps at the border between Germany and Austria (Fig. 1a). The altitude varies between 1035 m above sea level (asl) (Sägebach Spring) and 2230 m asl (summit of Mt. Hochifen). The Gottesacker karren field (Fig. 1b) covers an area of about 10 km². Geologically, the valley follows the contact between two tectonic units, the Helvetic Säntis Nappe, and the Flysch zone (Wagner 1950). The most important Helvetic rock formation is the Cretaceous Schrattenkalk limestone (75 – 125 m thick) which forms the surface of the Gottesacker terrain and acts as the main karst aquifer (Goldscheider 2005). The mountain range southeast of the valley is formed by low-permeability sedimentary rocks, including flysch and Amdener marl. It is characterized by low to moderate permeability and drains by surface runoff (Chen and Goldscheider 2014). The karst aquifer in the catchment of Aubach Spring (QA) and

Fig. 1 **a** Location map (*red arrow* indicates the location of the test site at the German - Austrian border in the northern Alps; *blue color* represents carbonate rocks; *red triangles* indicate the border between exposed and non-exposed karstifiable rocks (WOKAM, modified after Chen et al. 2017). **b** View of the test site, with the karst and surface catchment of the investigated springs; Subcatchment 1 is only drained by Sägebach Spring (QS), Subcatchment 2 is drained by Aubach Spring (QA) + QS, Subcatchment 3 is drained by Estavelle + QA + QS (basemap: Land Vorarlberg 2022). **c** Photo of the outlet of QA at a discharge of 3500 L/s. **d** Photo of the outlet of Sägebach Spring (QS) at a discharge of 450 L/s



Sägebach Spring (QS) (Fig. 1b-d) is recharged directly from precipitation and snowmelt (either diffuse or concentrated) and indirectly from surface streams that drain the southern part of the catchment area (Fig. 1b).

In the valley, two parallel drainage systems exist: a surface stream and an underground karst drainage system along the valley axis. An estavelle, together with a cave system, forms the hydraulic connection between the two flow systems. During high-flow conditions the estavelle acts as a karst spring and discharges up to 4000 L/s while during low-flow conditions, the surface stream sinks underground into the cave entrance with a rate of up to 500 L/s (Goldscheider 2005). Further downstream in the valley, the large, intermediate Aubach Spring (Fig. 1b, c) discharges up to 8000 L/s but runs completely dry during periods of drought and in winter. The largest permanent spring in the study area is the Sägebach Spring further downstream (Fig. 1b, d) which discharges up to 3500 L/s (Chen and Goldscheider 2014).

The nearest permanent weather station is in the Breitach valley (1140 m asl) and gives a mean annual rainfall of 1840 mm

and an air temperature of 5.7 °C. In the elevated parts of the study site, the precipitation is certainly higher and much of it is snow. Assuming a vertical temperature gradient of 0.6 °C/100 m (e.g., Veith 2002) a mean annual temperature of 0 °C is expected at an altitude of 2100 m. Due to intense karstification and the absence of soil and vegetation in the higher parts of the study site, the evapotranspiration is low and a large portion of rainfall contributes to the recharge and therefore to the discharge at the monitored springs.

Methods

Physicochemical data

Aubach Spring (QA) and Sägebach Spring (QS) were monitored from 01.07.2020 to 23.08.2020. Water temperature, electrical conductivity (EC) and turbidity were measured continuously at 5 to 15 min intervals using a GGUN-FL30 field fluorometer (detection limit 0.02 nephelometric turbidity units (NTU), Albillia Särl., Neuchâtel, Switzerland).

Water level data at Sägebach Spring was recorded with an OTT Orpheus Mini (OTT HydroMet GmbH, Kempten, Germany) water level logger. Discharge measurements were done using the salt dilution method with point injection. In total, 12 measurements were used to create a rating curve ($R^2 = 0.94$) to convert water levels into continuous discharge data. Water level (BD Sensors LMP308, Thierstein, Germany) at Aubach Spring has been continuously recorded since 1999 by the Water Management Department of Vorarlberg. Water level measurements were converted into discharge data using the rating curve of the Water Management Department of Vorarlberg. Their high-resolution data (15 min intervals) were used for this study.

Total organic carbon (TOC) and fecal indicator bacteria (*E. coli*)

Total organic carbon was detected using the flow-through field fluorometer GGUN-FL30 (Albillia Sàrl, Neuchâtel, Switzerland). It measures TOC by means of UV fluorescence. In addition, manual water samples were taken in 50 mL brown glass bottles and acidified with HCl (37 %) to stabilize the sample. TOC measurements were done in our laboratory at KIT, with a TOC analyzer (vario TOC cube, Elementar Analysensysteme GmbH, Hanau, Germany). These samples were analyzed in triplicate and the mean value was computed and used as TOC concentration. These measurements were utilized to create a rating curve for the field fluorometer to create continuous TOC data (Fig. S1 of the electronic supplementary material (ESM)).

Water samples for the subsequent analysis were taken manually or with an automatic sampler (Teledyne ISCO 3700, Lincoln, USA). For the analysis of fecal indicator bacteria, 159 water samples were taken each at Aubach Spring and Sägebach Spring in 3–8-hour intervals; 100 mL bottles containing sodium thiosulfate were filled. The bottles were stored in the dark at 4°C until analysis for total coliforms and *E. coli*, which is widely accepted as fecal indicator (e.g., Edberg et al. 2000). Bacteria were identified as the most probable number (MPN) per 100 mL following the Colisure-Quanty-Tray/2000 method (IDEXX Laboratories Inc., Westbrook, USA), which is approved by the U.S. Environmental Protection Agency and included in the Standard Methods for Examination of Water and Wastewater. The microbial detection range of this testing method is from 1–2419 MPN/100 ml. Where an exceedance of this value was expected, the samples were diluted with ultrapure water.

Enzymatic activity of β -D-glucuronidase and ATP

The measurement of the enzymatic activity is based on the increase of the fluorescence intensity, resulting from the activity of β -D-glucuronidase (GLUC) and, hence, the accumulation of the highly fluorescent reaction product

4-Methylumbelliferone (Stadler et al. 2016). The measurements were performed with a mobile instrument (ColiMinder, VWMS GmbH, Zwerndorf, Austria) that was automatically cleaned before and after each measurement. A detailed description of the device can be found in Koschelnik et al. (2015). For each measurement, a fresh, unfiltered water sample is pumped into the measurement chamber, where it is mixed with a defined buffer and the substrate solution (QuickDetect Reagents, VWMS GmbH). Because the maximal GLUC activity can be observed at 44 °C (George et al. 2000), the solution is preheated to a constant temperature of 44 °C before the measurement cycle is started automatically. Results of GLUC activity measurements are expressed in Modified Fishman Units (MFU) following the standard Sigma Quality Control Test Procedure (Sigma-Aldrich 1998). The measurement interval can be set up manually. A complete measurement cycle takes approximately 20 min. The device is equipped with an internal battery, but in this case, the ColiMinder was set up at the Sägebach Spring where power supply was available.

Adenosine triphosphate (ATP) as an indicator of water hygiene was previously used especially for drinking water and in the food industry (e.g. Hansen et al. 2019). In this study, the spring water quality was determined using the Hygiene AquaSnap Total test kits (Hygiene LLC, Camarillo, USA). The AquaSnap Total test measures both, microbial (living cells and particulate matter) and free ATP (non-microbial or dead cells) in water. The test device contains a detergent to release ATP that is bound to microbial and non-microbial organic matter. The dipper of the test device collects 100 μ L of water, then the contained luciferase enzyme comes into contact with ATP and produces a bioluminescence reaction. The light emitted from this reaction can be measured and was quantified with the Hygiene Ensure Touch luminometer (limit of detection (LOD) = 1 relative light unit (RLU)).

Fluorescence spectroscopy

Colored dissolved organic matter (CDOM) is the optically measurable component of dissolved organic matter in water. Excitation-emission matrices (EEMs) are the state-of-the-art measurement technique for fDOM fluorescence (fluorescent dissolved organic matter). EEMs were obtained using the Aqualog fluorometer (Horiba Ltd., Kyoto, Japan). An EEM is acquired by simultaneous scanning of the excitation spectrum and the fluorescence emission spectrum at each excitation wavelength. The field samples were analyzed in a quartz cuvette with a path length of 10 mm maintained at a constant temperature of 20 °C in the laboratory. The cuvette was cleaned after each measurement. For each sample, a simultaneous scan of excitation and emission wavelength from 240 to 600 nm with 5 nm intervals was performed. First and second order Rayleigh scattering was removed by nullifying the signal intensities of

the Rayleigh lines. The Raman scatter line is removed by subtracting a blank measurement from the sample EEM. EEMs were corrected for inner filter effects (IFE) using the parallel absorbance measurement from the blank and from the sample (Gilmore 2011). The fluorescence intensities were determined with the peak-picking technique (Coble 1996). Usually, several peaks can be observed in samples from karst spring waters, which are referred to as follows: Peak A (humic-like substances) was identified at excitation wavelength (ex) 240–260 nm and emission wavelength (em) 400–480 nm in all samples, peak T (protein-like fluorescence) was identified at ex 270–280 nm and em 300–350 nm, which is in accordance with Coble (1996) and Frank et al. (2018). The samples were not diluted.

Particle-size distribution

Particle-size distribution (PSD) was measured using two portable PCSS Fluid Lite particle counters (Markus Klotz GmbH, Bad Liebenzell, Germany). The PCSS Fluid Lite counts suspended particles in the range of 0.9–400 μm and groups them into 16 definable size classes. The automated measuring procedure starts with a rinsing process followed by the actual measurement in which 10 mL of the sample water passes through a small glass tube. The tube is irradiated by a laser beam and the contained particles cause a decrease in the laser light at the detector. The instrument assumes an equivalent spherical diameter of the particle and thereby the size of the particle. The particle counters were placed directly at the two springs. In all, 16 particle size classes were measured but only the small size classes were of special interest: 0.9–1.0 μm (hereinafter 1.0 μm), 1.1–2.0 μm (2.0 μm), 2.1–3.0 μm (3.0 μm), 3.1–4.0 μm (4.0 μm) and 4.1–5.0 μm (5.0 μm). These size fractions have a higher mobility compared to larger ones and can be transported through the whole aquifer. They are well suited to be compared to *E. coli* which have a size of about 1–3 μm (Reshes et al. 2008) and are likely to show similar mobility.

In the measurements taken as part of this study, the small particle-size classes 1 and 2 μm reached values of approximately 3 million particles per 10 mL and about 1.2 million particles per 10 mL. When the used particle counter reaches a cumulative particle amount of over 1.2 million particles per 10 mL, coincidence occurs. Because of this, the particle fractions 1 and 2 μm were correlated with turbidity measurements ($R^2 = 0.9$) and the values for these two particle-size classes were used for further analysis. In this case, it was assumed that the fraction between the different size classes remained approximately the same during different turbidity levels.

Hydrochemical investigations

During the detailed monitoring periods at both springs, water samples were collected in 3- to 8-hour intervals,

manually and with an automatic sampler. For the analysis of anions, 50 mL PE bottles were used and 15 mL PP tubes for the analysis of cations. Water samples were filtered with cellulose acetate membrane filters (0.45 μm , 25 mm, Sartorius AG, Göttingen Germany). The samples for the analysis of cations were acidified with HNO_3 (65 %) on-site and all samples were stored at 4 °C until the analysis in the laboratory. Alkalinity was measured as triplicate by volumetric titration on-site using an alkalinity test (Merck KGaA, Darmstadt, Germany) and the mean value was taken. All other anions were measured using an IC system (Dionex ICS-2100, Sunnyvale, USA). The LODs for the anions are as follows: $\text{Cl}^- = 0.34 \text{ mg/L}$, $\text{SO}_4^{2-} = 0.79 \text{ mg/L}$, $\text{NO}_3^- = 0.34 \text{ mg/L}$. All cations were analyzed with an ICP-MS 7800 (Agilent Technologies, Santa Clara, USA). The LODs for the cations are as follows: $\text{Na}^+ = 1.04 \text{ }\mu\text{g/L}$; $\text{K}^+ = 4.46 \text{ }\mu\text{g/L}$; $\text{Ca}^{2+} = 64.24 \text{ }\mu\text{g/L}$; $\text{Mg}^{2+} = 2.27 \text{ }\mu\text{g/L}$. For Aubach Spring, the ion charge balance error, calculated according to DIN 38402-62 (2014), is -2.05 % and for Sägebach Spring, the calculated charge balance error is 0.88 %.

Results and discussion

Time series of Aubach and Sägebach springs

The investigations for this study were carried out from 30.06.2020 to 25.08.2020, a period that was not affected by snowmelt in the catchment. At both springs, distinct reactions of the measured parameters after rainfall events were recorded for all measured parameters. At Aubach Spring, minimum discharge during the investigation period was 149 L/s while the minimum discharge at Sägebach Spring was 204 L/s (Table 1).

Maximum discharge values were recorded after a heavy rain event on 04.08.2020 with 6183 L/s (Aubach spring) and 3670 L/s (Sägebach spring) respectively. The values of electrical conductivity (EC) show an inverted reaction compared to the discharge (Figs. 2 and 3). Minimum values for EC were 190 $\mu\text{S/cm}$ at Aubach Spring and 166 $\mu\text{S/cm}$ at Sägebach Spring while 276 $\mu\text{S/cm}$ and 227 $\mu\text{S/cm}$ respectively were the maximum measured values. The EC minimum represents fairly well the real arrival of the event water, which is also supported by many other studies (e.g. Frank et al. 2018; Linan Baena et al. 2009; Nannoni et al. 2020) which also found negative correlations with a slight time-lag between EC and discharge.

Large turbidity peaks were recorded at both springs on 03.08.2020 and 04.08.2020 and on 17.08.2020 and 18.08.2020 while Sägebach Spring shows another large turbidity peak on 23.07.2020 (Figs. 2 and 3). This peak is believed to be caused by an extremely focused rain event which occurred in sub-catchment 1 (Fig. 1b) during the evening of 22 July 2020 and therefore only affected Sägebach spring.

Table 1 Summary statistics for discharge, water temperature, electrical conductivity (EC), turbidity, total organic carbon (TOC), bacteria, fluorescence peaks A and T (A.U. arbitrary unit) and ATP total for Aubach and Sägebach spring for the whole investigation period. S.D. standard deviation; CV coefficient of variation

| | | Aubach Spring | Sägebach Spring |
|-------------------|------------------|---------------|-----------------|
| Discharge | <i>n</i> | 5062 | 5098 |
| | Min. [L/s] | 149 | 204 |
| | Max. [L/s] | 6183 | 3670 |
| | Mean [L/s] | 677 | 463 |
| | S.D. | 919 | 812 |
| | CV [%] | 136 | 162 |
| Water Temperature | <i>n</i> | 11707 | 11741 |
| | Min. [°C] | 5.1 | 5.4 |
| | Max. [°C] | 6.8 | 8.4 |
| | Mean [°C] | 6.0 | 5.6 |
| | S.D. | 0.3 | 0.1 |
| | CV [%] | 5.5 | 2.7 |
| EC | <i>n</i> | 11707 | 11741 |
| | Min. [μS/cm] | 190 | 166 |
| | Max. [μS/cm] | 276 | 227 |
| | Mean [μS/cm] | 245 | 204 |
| | S.D. | 17 | 13 |
| | CV [%] | 7 | 6 |
| Turbidity | <i>n</i> | 11707 | 5609 |
| | Min. [NTU] | 0.1 | 0.0 |
| | Max. [NTU] | 23.9 | 27.2 |
| | Mean [NTU] | 0.5 | 0.9 |
| | S.D. | 1.6 | 2.5 |
| | CV [%] | 342.0 | 262.8 |
| TOC | <i>n</i> | 11707 | 11746 |
| | Min. [mg/L] | 0.7 | 0.9 |
| | Max. [mg/L] | 4.5 | 7.1 |
| | Mean [mg/L] | 1.4 | 2.3 |
| | S.D. | 0.6 | 1.1 |
| | CV [%] | 43.1 | 47.6 |
| <i>E. coli</i> | <i>n</i> | 159 | 159 |
| | Min. [MPN/100mL] | 25 | 19 |
| | Max. [MPN/100mL] | 3466 | 3973 |
| | Mean [MPN/100mL] | 311 | 273 |
| | S.D. | 548 | 474 |
| | CV [%] | 176 | 176 |
| Peak A | <i>n</i> | 112 | 105 |
| | Min. [A.U.] | 1136 | 1637 |
| | Max. [A.U.] | 6401 | 9204 |
| | Mean [A.U.] | 2097 | 3202 |
| | S.D. | 990 | 1572 |
| | CV [%] | 47 | 50 |
| Peak T | <i>n</i> | 112 | 105 |
| | Min. [A.U.] | 228 | 299 |
| | Max. [A.U.] | 2139 | 1396 |
| | Mean [A.U.] | 597 | 645 |
| | S.D. | 288 | 336 |
| | CV [%] | 51 | 49 |
| ATP total | <i>n</i> | 112 | 113 |
| | Min. [RLU] | 13 | 6 |
| | Max. [RLU] | 614 | 972 |
| | Mean [RLU] | 101 | 82 |
| | S.D. | 111 | 119 |
| | CV [%] | 110 | 145 |

Total organic carbon (TOC) varied between 0.7 and 4.5 mg/L at Aubach Spring and between 0.9 and 7.1 mg/L at Sägebach Spring (Table 1). The evolution of *E. coli* shows a similar pattern at both springs and the values at Aubach Spring varied between 25 and 3466 MPN/100 mL while the values at Sägebach Spring varied between 15 and 3973 MPN/100 mL (Table 1). The maximum bacteria levels at Sägebach Spring were measured after the heavy rain event on 02 August 2020 and 03 August 2020, where also maximum discharge, maximum TOC and minimum EC were recorded (Fig. 3).

Maximum *E. coli* values at Aubach Spring were detected on 17 August 2020, after a rather small rain event. While discharge only increased by about 500 L/s and EC only decreased by 25 $\mu\text{S}/\text{cm}$, the maximum turbidity peak was recorded with 23.9 NTU after this event (Fig. 2).

Detailed monitoring campaigns

For a more detailed investigation of bacterial and particle dynamics, detailed monitoring was done from 22.07.2020

Fig. 2 Temporal patterns of discharge, EC, and turbidity, together with TOC, fecal indicator bacteria *E. coli* and rainfall data from a nearby weather station for Aubach Spring. The grey bars indicate the detailed monitoring periods

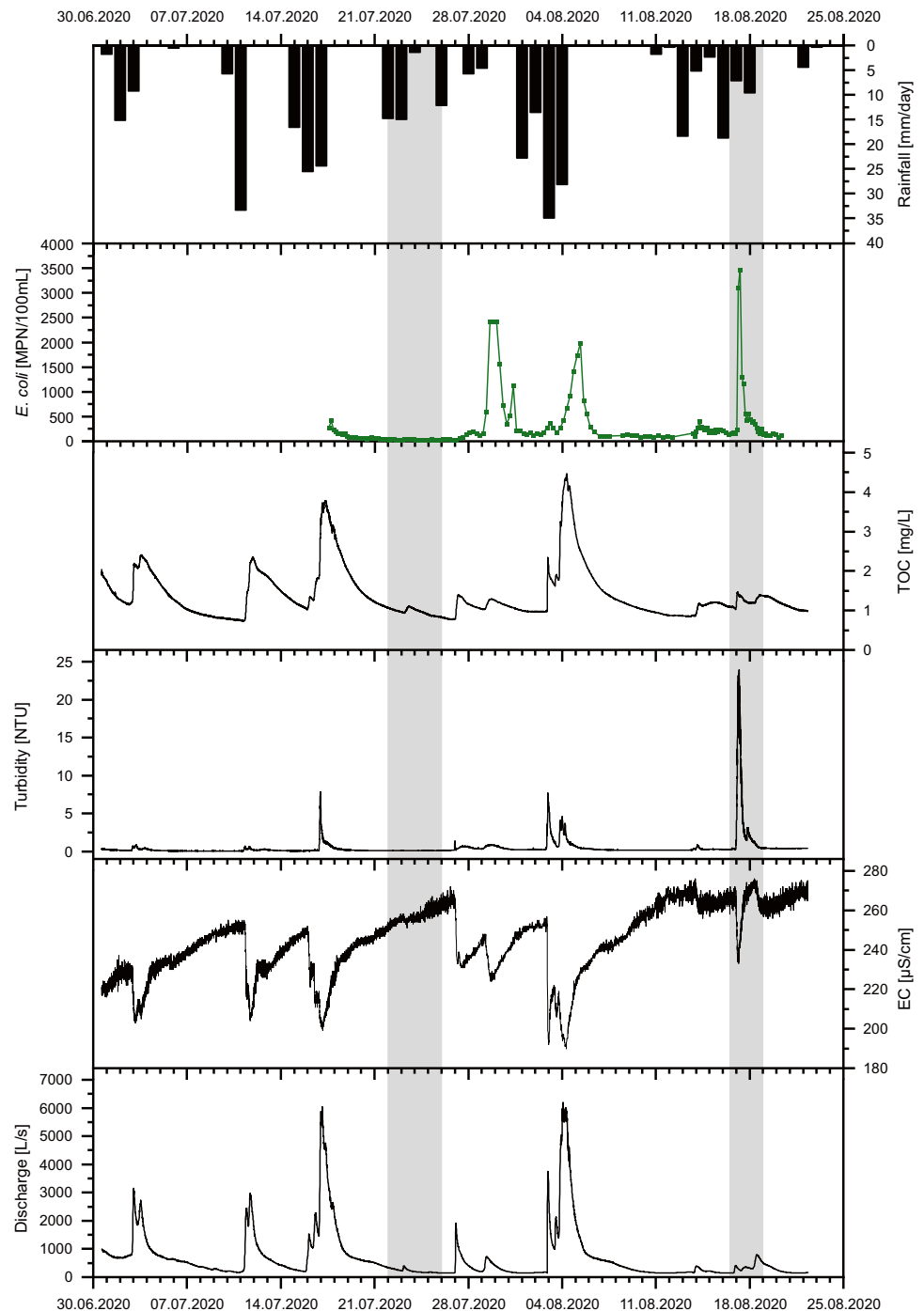
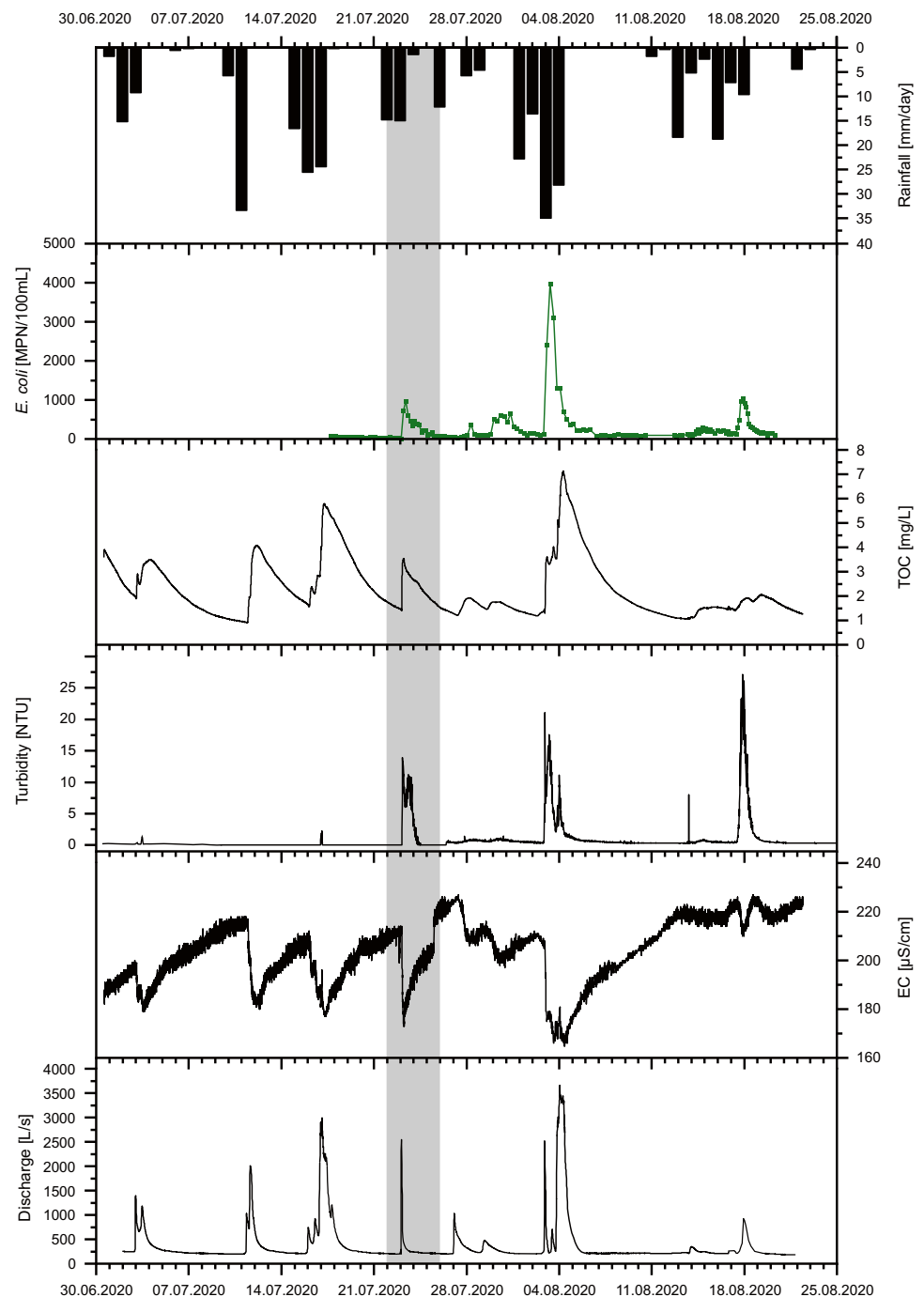


Fig. 3 Temporal patterns of discharge, EC, turbidity, TOC and *E. coli* together with rainfall data from a nearby weather station for Sägebach Spring. The grey bar indicates the detailed monitoring period at Sägebach Spring (same period as for Aubach Spring in Fig. 2)



to 26.07.2020, directly after a rainfall event. Because of the extremely focused rain event in Subcatchment 1, Aubach Spring showed no reaction (see Fig. 2 and Fig. S2 of the ESM) therefore, another detailed investigation at Aubach Spring was carried out from 16 August 2020 to 19 August 2020. In addition to the already mentioned parameters, PSD, natural fluorescence (peaks A and T) and ATP total were measured at Aubach Spring. Additionally, the enzymatic activity of β -D-glucuronidase (GLUC) was measured with the ColiMinder device at Sägebach Spring. The temporal

patterns for the detailed monitoring periods at Sägebach Spring are given in Fig. 4 and for Aubach Spring in Fig. 5.

During the 22 July 2020 to 26 July 2020 event monitored at Sägebach Spring, the particle-size classes, GLUC activity and turbidity clearly show two identifiable peaks. Natural fluorescence, *E. coli*, and ATP total only show one peak. The single peaks of *E. coli*, natural fluorescence and ATP total seem to appear at the same time as the second peak of particles and turbidity. The steep increase of particle concentrations and turbidity is most probably caused by a hydraulic pressure pulse

triggered by the rain event. This led to a remobilization of sediments from inside the karst network which results in the first peak of particles and turbidity. Further, the second peak can be attributed to the arrival of turbid water from the land surface (allochthonous) which is enriched with bacteria and other organic content flushed into the karst aquifer from the rain event. A similar behavior was also observed in previous studies at other investigated karst sites (e.g. Pronk et al. 2009). In this case, at Sägebach Spring, the parameters turbidity and PSD can act as an early-warning system for fecal contamination because the bacterial contamination occurs during the second peak of these parameters. As mentioned previously, both turbidity and PSD can be measured in near real-time and automatically, while e.g. ATP samples have to be taken manually.

During the monitoring at Aubach Spring from 16 August 2020 to 19 August 2020 (Fig. 5), concentrations in all particle-size classes, turbidity, natural fluorescence, ATP total and *E. coli* show a simultaneous increase and the peak was reached almost at the same time. The increase of these parameters occurs with a time lag of about three hours compared to the increase of discharge which is most probably caused by the piston effect (Ravbar et al. 2011). While all parameters except the direct determination of *E. coli* can be measured in near real time, these parameters are potentially suitable as real time indicators for bacterial contamination at Aubach Spring. As the increase of all parameters occurs simultaneously but with a time lag relative to discharge, discharge can be used as an early-warning parameter at this spring. Interesting to note is also, that at Aubach Spring:

- The parameter TOC seems to reflect both fluorescence parameters (peak A and peak T) as it also shows a slight double peak pattern (in contrast to Sägebach Spring, whereas TOC clearly has only one peak).
- The measured particles seem to be completely flushed out of the system within approximately 3 days for Sägebach Spring and within less than 2 days at Aubach Spring after the respective rain event.

A correlation table for all parameters investigated during the detailed monitoring at both springs, together with their significance is given in Fig. S3 of the ESM. At Sägebach Spring, the best correlation with *E. coli* was found with the particle-size classes 2, 3 and 4 μm (with a Spearman's rank correlation p of 0.91–0.93) and with peak T fluorescence. The correlation with GLUC activity is also significant ($p = 0.88$).

For both storm events, the hydrochemical behavior of Aubach Spring and Sägebach Spring, together with all measured parameters, are given in Fig. 6.

At both springs, many parameters, including all particle sizes, bacteria and organic material show a strong increase after the rain events (at Aubach Spring on 17.08.2020 at 01:30 and at Sägebach Spring on 23.07.2020 at 04:00 (Fig. 6). This suggests that these substances are mobilized by the respective rain events

and transported to the spring. In contrast, anions and cations, as well as EC, show a sharp decrease after the respective rain events because of dilution with fresh and low-mineralized water entering the karst system and reaching both springs.

Conclusions

Two alpine karst springs in Austria were monitored to gain a more detailed knowledge about the spring dynamics occurring in conduit-dominated karst aquifer systems. During high-resolution monitoring of a storm event, new parameters were tested to check and validate their use as real-time or early-warning parameters for bacterial contamination at karst springs. To characterize transport processes within the aquifer and to determine the reaction of the springs to rainfall events, particle-size distribution and physicochemical parameters were measured. The results show:

- A fast and marked response of these parameters after rainfall events was observed which demonstrates a conduit-dominated karst system with fast flow components.
- A high correlation and a simultaneous response to the rain event of all recorded water quality parameters was found.
- While conventional *E. coli* determination methods need about 24 h for final results, TOC, the particle load and the particle-size distribution can be measured in near real-time, and therefore can be used as a real-time indication system for bacterial contamination.

In addition to the already-mentioned parameters, a focus of the investigation was the application of the ColiMinder device and the use of the GLUC activity as a possible surrogate parameter for *E. coli*. GLUC activity results show:

- A double peak pattern for particles and turbidity after the rain event at Sägebach Spring (QS), while TOC, conventional *E. coli* determinations, and natural fluorescence only show one peak, concurrent with the second peak of TOC, *E. coli* and natural fluorescence.
- The best correlations for *E. coli* were found with small particle-size classes, peak T fluorescence and GLUC activity. Therefore, particle load and particle-size distribution and/or turbidity, together with GLUC activity are suitable parameters for an early-warning system regarding bacterial contamination, because the real *E. coli* contamination occurs during the second peak of these parameters.
- At least at the event scale, that GLUC activity can be used as a real-time indicator of fecal contamination because GLUC measurements with the ColiMinder take about 25 minutes compared to 24 h for conventional *E. coli* determinations. However, since the ColiMinder does

Fig. 4 Temporal patterns of discharge, EC, particle size classes 1–5 μm , turbidity, β -D-glucuronidase activity, TOC, *E. coli*, and fluorescence peaks A and T for Sägebach Spring

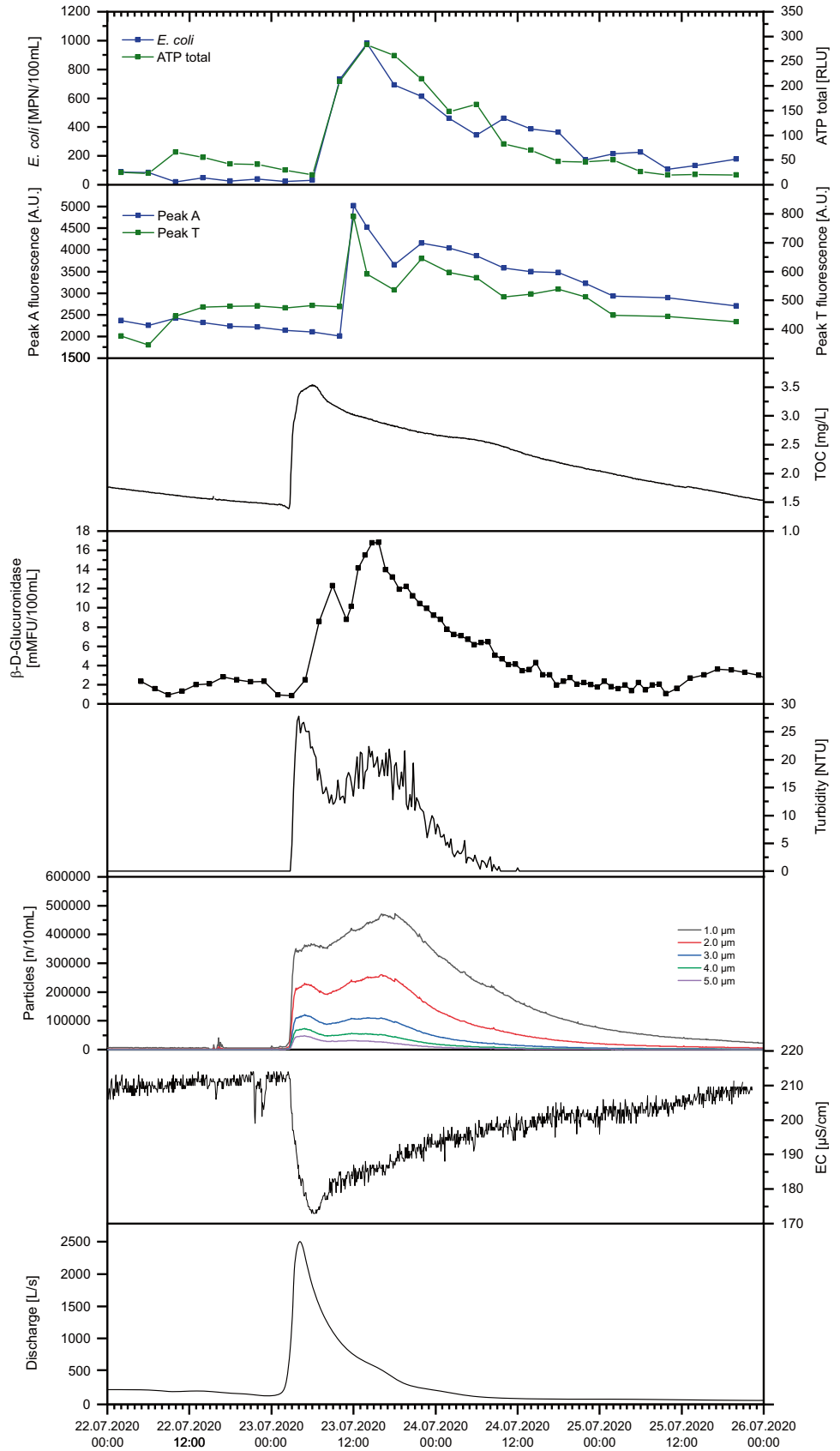
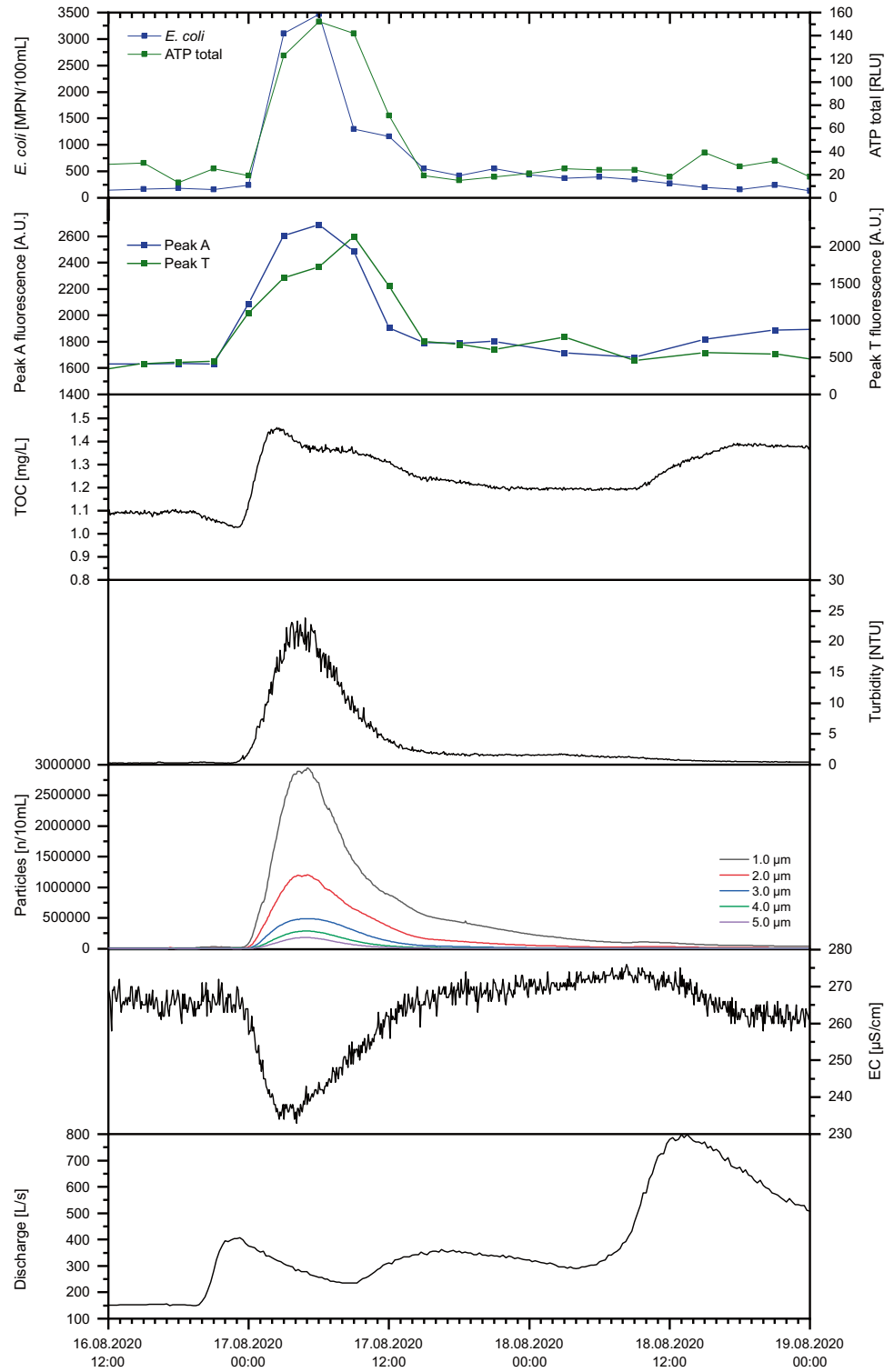


Fig. 5 Temporal patterns of discharge, EC, particle size classes 1–5 μm , turbidity, TOC, fluorescence peaks A and T, together with the determined *E. coli* values for the Aubach Spring

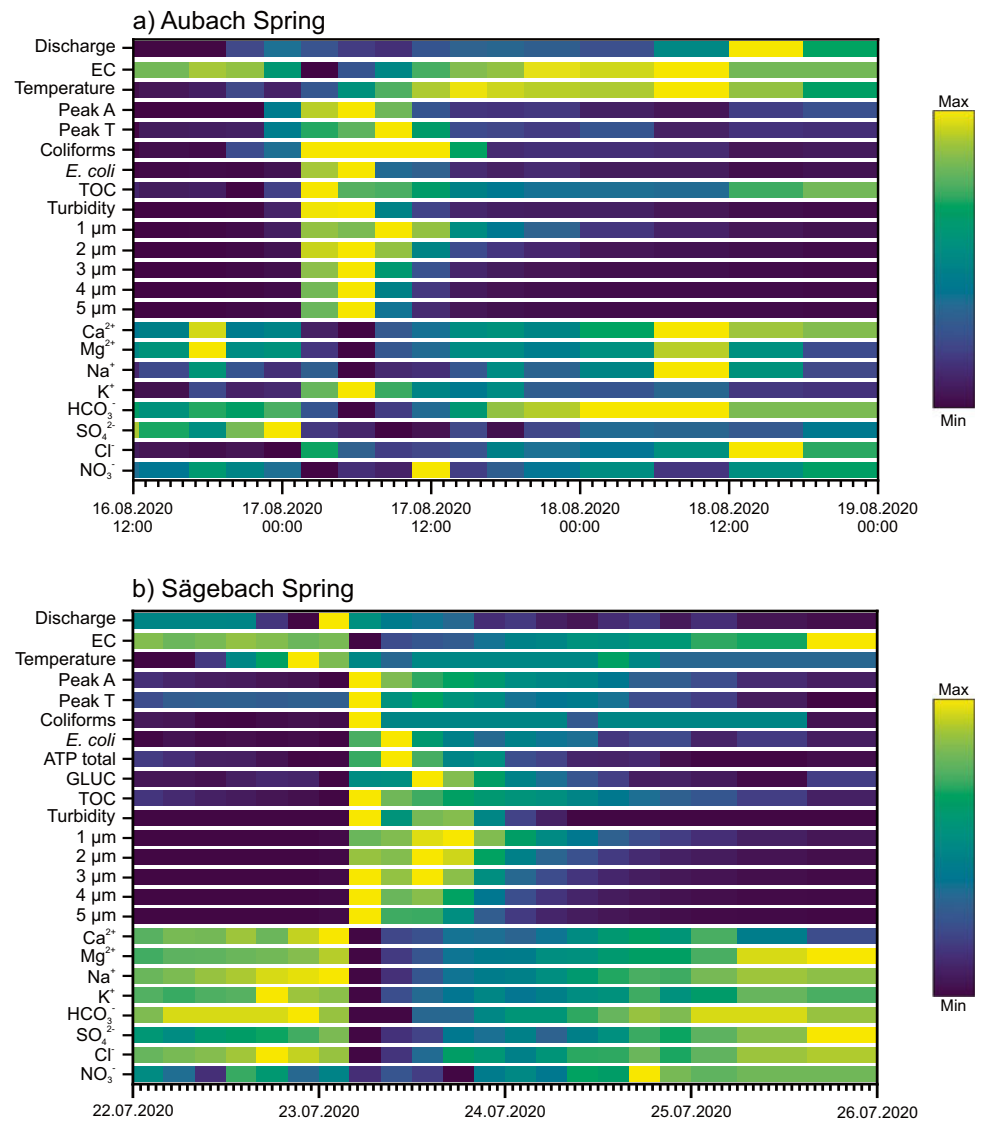


not deliver the actual *E. coli* quantity, it cannot substitute conventional determination methods.

At both springs, this study clearly shows the need for high-resolution monitoring to record the contamination

dynamics in this karst aquifer. All measured parameters showed a fast and marked reaction to rain events, so it is especially important to determine parameters which are related to fecal contamination and can be measured in near real-time.

Fig. 6 Temporal patterns of all parameters including cations and anions shown as a color map for (a) Aubach Spring and (b) Sägebach Spring



On the one hand, rain events lead to a mobilization, especially of particles, organic material and bacteria, while on the other hand rain events lead to a dilution effect, which mainly affects the major anions and cations. This effect was also observed at a different karst spring by Stange and Thiem (2020). These results presented in this study highlight the vulnerability of karst aquifers, especially after rain events and demonstrate the need for advanced measurement techniques and novel parameters to detect and predict fecal contamination, which is important in regard to time-consuming conventional bacterial detection methods.

Supplementary Information The online version contains supplementary material available at <https://doi.org/10.1007/s10040-022-02556-8>.

Acknowledgments The authors acknowledge the financial support of the Federal Ministry of Education and Research (BMBF) and the European Commission through the Partnership for Research and Innovation in the Mediterranean Area (PRIMA) programme under Horizon 2020 (KARMA Project, grant agreement number 01DH19022A). The authors thank the Water Management Department of the Vorarlberg State Administration, especially Clemens Mathis, for providing the discharge data for Aubach Spring. Special thanks are also given to Karl Kessler and Philip Engel for providing logistical support and help during the field work, to Roman Gural for granting access to the Sägebach Spring, and to KIT laboratory staff Daniela Blank, Christine Buschhaus and Christine Roske-Stegemann. Further thanks go to Joachim Schrautzer (Kiel University) for providing rainfall data for the area from their weather station and to Benjamin Tobin (Lexington, USA) for language checks on the original manuscript.

Funding Open Access funding enabled and organized by Projekt DEAL.

Open Access This article is licensed under a Creative Commons Attribution 4.0 International License, which permits use, sharing, adaptation, distribution and reproduction in any medium or format, as long as you give appropriate credit to the original author(s) and the source, provide a link to the Creative Commons licence, and indicate if changes were made. The images or other third party material in this article are included in the article's Creative Commons licence, unless indicated otherwise in a credit line to the material. If material is not included in the article's Creative Commons licence and your intended use is not permitted by statutory regulation or exceeds the permitted use, you will need to obtain permission directly from the copyright holder. To view a copy of this licence, visit <http://creativecommons.org/licenses/by/4.0/>.

References

- Abia ALK, Ubomba-Jaswa E, Genthe B, Momba MNB (2016) Quantitative microbial risk assessment (QMRA) shows increased public health risk associated with exposure to river water under conditions of riverbed sediment resuspension. *Sci Total Environ* 566–567:1143–1151. <https://doi.org/10.1016/j.scitotenv.2016.05.155>
- Bakalowicz M (2005) Karst groundwater: a challenge for new resources. *Hydrogeol J* 13:148–160. <https://doi.org/10.1007/s10040-004-0402-9>
- Baker A, Inverarity R (2004) Protein-like fluorescence intensity as a possible tool for determining river water quality. *Hydrol Process* 18:2927–2945. <https://doi.org/10.1002/hyp.5597>
- Baker A, Lamont-Black J (2001) Fluorescence of Dissolved Organic Matter as a Natural Tracer of Ground Water. *Ground Water* 39:745–750. <https://doi.org/10.1111/j.1745-6584.2001.tb02365.x>
- Chen Z, Goldscheider N (2014) Modeling spatially and temporally varied hydraulic behavior of a folded karst system with dominant conduit drainage at catchment scale, , Hochifèn–Gottesacker, Alps. *J Hydrol* 514:41–52. <https://doi.org/10.1016/j.jhydrol.2014.04.005>
- Chen Z, Auler AS, Bakalowicz M, David D, Griger F, Hartmann J, Jiang G, Moosdorf N, Richts A, Stevanovic Z, Veni G, Goldscheider N (2017) The World Karst Aquifer Mapping project: concept mapping procedure and map of Europe. *Das Welt-Karstaquifer-Kartierprojekt: Konzept Vorgehensweise und Europakarte. Le programme de la Carte Mondiale des Aquifères Karstiques: concept procédure de cartographie et carte de l'Europe. Mapping: concepto procedimiento de mapeo y mapa de Europa. 世界岩溶含水层分布图:制图的概念、流程以及欧洲地区样图. Projeto Mapeamento Global de Aquíferos Cársticos (WOKAM): conceito procedimentos adotados e mapa da Europa.* *Hydrogeol J* 25(3):771–785. <https://doi.org/10.1007/s10040-016-1519-3>
- Coble PG (1996) Characterization of marine and terrestrial DOM in seawater using excitation-emission matrix spectroscopy. *Mar Chem* 51:325–346. [https://doi.org/10.1016/0304-4203\(95\)00062-3](https://doi.org/10.1016/0304-4203(95)00062-3)
- Determann S, Lobbes JM, Reuter R, Rullkötter J (1998) Ultraviolet fluorescence excitation and emission spectroscopy of marine algae and bacteria. *Mar Chem* 62:137–156. [https://doi.org/10.1016/S0304-4203\(98\)00026-7](https://doi.org/10.1016/S0304-4203(98)00026-7)
- Dussart-Baptista L, Massei N, Dupont J-P, Jouenne T (2003) Transfer of bacteria-contaminated particles in a karst aquifer: evolution of contaminated materials from a sinkhole to a spring. *J Hydrol* 284:285–295. <https://doi.org/10.1016/j.jhydrol.2003.08.007>
- Edberg SC, Rice EW, Karlin RJ, Allen MJ (2000) *Escherichia coli*: the best biological drinking water indicator for public health protection. *J Appl Microbiol* 88:106–116. <https://doi.org/10.1111/j.1365-2672.2000.tb05338.x>
- Ender A, Goepfert N, Grimmeisen F, Goldscheider N (2017) Evaluation of β -d-glucuronidase and particle-size distribution for microbiological water quality monitoring in Northern Vietnam. *Sci Total Environ* 580:996–1006. <https://doi.org/10.1016/j.scitotenv.2016.12.054>
- Farnleitner AH, Hocke L, Beiwl C, Kavka GG, Mach RL (2002) Hydrolysis of 4-methylumbelliferyl- β -d-glucuronide in differing sample fractions of river waters and its implication for the detection of fecal pollution. *Water Res* 36(4):975–981. [https://doi.org/10.1016/S0043-1354\(01\)00288-3](https://doi.org/10.1016/S0043-1354(01)00288-3)
- Fellman JB, Hood E, D'Amore DV, Edwards RT, White D (2009) Seasonal changes in the chemical quality and biodegradability of dissolved organic matter exported from soils to streams in coastal temperate rainforest watersheds. *Biogeochemistry* 95:277–293. <https://doi.org/10.1007/s10533-009-9336-6>
- Ferguson AS, Layton AC, Mailloux BJ, Culligan PJ, Williams DE, Smartt AE, Saylor GS, Feighery J, McKay LD, Knappett PSK, Alexandrova E, Arbit T, Emch M, Escamilla V, Ahmed KM, Alam MJ, Streatfield PK, Yunus M, van Geen A (2012) Comparison of fecal indicators with pathogenic bacteria and rotavirus in groundwater. *Sci Total Environ* 431:314–322. <https://doi.org/10.1016/j.scitotenv.2012.05.060>
- Fiksdal L, Tryland I (2008) Application of rapid enzyme assay techniques for monitoring of microbial water quality. *Curr Opin Biotech* 19:289–294. <https://doi.org/10.1016/j.copbio.2008.03.004>
- Ford D, Williams P (2007) *Karst Hydrogeology and Geomorphology*, John Wiley & Sons Ltd
- Frank S, Goepfert N, Goldscheider N (2018) Fluorescence-based multi-parameter approach to characterize dynamics of organic carbon, faecal bacteria and particles at alpine karst springs. *Sci Total Environ* 615:1446–1459. <https://doi.org/10.1016/j.scitotenv.2017.09.095>
- George I, Petit M, Servais P (2000) Use of enzymatic methods for rapid enumeration of coliforms in freshwaters. *J Appl Microbiol* 88:404–413. <https://doi.org/10.1046/j.1365-2672.2000.00977.x>
- Gilmore AM, (2011) *Water Quality Measurements with HORIBA Jobin Yvon Fluorescence Instrumentation*
- Goldscheider N (2005) Fold structure and underground drainage pattern in the alpine karst system Hochifèn-Gottesacker. *Eclogae geol. Helv.* 98:1–17. <https://doi.org/10.1007/s00015-005-1143-z>
- Hansen CB, Kerrouche A, Tatari K, Rasmussen A, Ryan T, Summersgill P, Desmulliez MPY, Bridle H, Albrechtsen HJ (2019) Monitoring of drinking water quality using automated ATP quantification. *J Microbiol Meth* 165. <https://doi.org/10.1016/j.mimet.2019.105713>
- Heery B, Briciu-Burghina C, Zhang D, Duffy G, Brabazon D, O'Connor N, Regan F (2016) ColiSense, today's sample today: A rapid on-site detection of β -d-Glucuronidase activity in surface water as a surrogate for *E. coli*. *Talanta* 148:75–83. <https://doi.org/10.1016/j.talanta.2015.10.035>
- Koschelnic J, Vogl W, Epp M, Lackner M (2015) Rapid analysis of β -D-glucuronidase activity in water using fully automated technology. Presented at the Water resources management 2015, A Coruña, Spain, pp. 471–481, <https://doi.org/10.2495/WRM150401>
- Kralik M (2001) *Strategie zum Schutz der Karstwassergebiete in Österreich.* Umweltbundesamt GmbH, Wien
- Kresic N, Stevanovic Z (2010) *Groundwater Hydrology of Springs. Management, and Sustainability*, Elsevier, Engineering Theory, p 592p
- Linan Baena C, Andreo B, Mudry J, Carrasco Cantos F (2009) Groundwater temperature and electrical conductivity as tools to characterize flow patterns in carbonate aquifers: The Sierra de las Nieves karst aquifer, southern Spain. *Hydrogeol J* 17:843–853. <https://doi.org/10.1007/s10040-008-0395-x>
- Mahler BJ, Personné J-C, Lods GF, Drogue C (2000) Transport of free and particulate-associated bacteria in karst. *J Hydrol* 238:179–193. [https://doi.org/10.1016/S0022-1694\(00\)00324-3](https://doi.org/10.1016/S0022-1694(00)00324-3)

- Nannoni A, Vigna B, Fiorucci A, Antonellini M, De Waele J (2020) Effects of an extreme flood event on an alpine karst system. *J Hydrol* 590. <https://doi.org/10.1016/j.jhydrol.2020.125493>
- Pronk M, Goldscheider N, Zopfi J (2006) Dynamics and interaction of organic carbon, turbidity and bacteria in a karst aquifer system. *Hydrogeol J* 14(4):473–484. <https://doi.org/10.1007/s10040-005-0454-5>
- Pronk M, Goldscheider N, Zopfi J (2007) Particle-Size Distribution As Indicator for Fecal Bacteria Contamination of Drinking Water from Karst Springs. *Environ. Sci. Technol.* 41:8400–8405. <https://doi.org/10.1021/es071976f>
- Pronk M, Goldscheider N, Zopfi J, Zwahlen F (2009) Percolation and particle transport in the unsaturated zone of a karst aquifer. *Groundwater* 47:3. <https://doi.org/10.1111/j.1745-6584.2008.00509.x>
- Quiers M, Batiot-Guilhe C, Bicalho CC, Perrette Y, Seidel J-L, Van Exter S (2014) Characterisation of rapid infiltration flows and vulnerability in a karst aquifer using a decomposed fluorescence signal of dissolved organic matter. *Environ Earth Sci* 71:553–561. <https://doi.org/10.1007/s12665-013-2731-2>
- Ravbar N, Engelhardt I, Goldscheider N (2011) Anomalous behaviour of specific electrical conductivity at a karst spring induced by variable catchment boundaries: the case of the Podstenjšek spring. Slovenia. *Hydrol Process* 25:2130–2140. <https://doi.org/10.1002/hyp.7966>
- Reshes G, Vanounou S, Fishov I, Feingold M (2008) Cell Shape Dynamics in *Escherichia coli*. *Biophys J* 94:251–264. <https://doi.org/10.1529/biophysj.107.104398>
- Sigma-Aldrich (1998) Enzymatic Assay of b-Glucuronidase (EC 3.2.1.31) from *E. coli*. Saint Luis, Missouri
- Sorensen JPR, Lapworth DJ, Marchant BP, Nkhuwa DCW, Pedley S, Stuart ME, Bell RA, Chirwa M, Kabika J, Liemisa M, Chibesa M (2015) In-situ tryptophan-like fluorescence: A real-time indicator of faecal contamination in drinking water supplies. *Water Res* 81:38–46. <https://doi.org/10.1016/j.watres.2015.05.035>
- Sorensen JPR, Vivanco A, Ascott MJ, Gooddy DC, Lapworth DJ, Read DS, Rushworth CM, Bucknall J, Herbert K, Karapanos I, Gumm LP, Taylor RG (2018) Online fluorescence spectroscopy for the real-time evaluation of the microbial quality of drinking water. *Water Res* 137:301–309. <https://doi.org/10.1016/j.watres.2018.03.001>
- Stadler P, Blöschl G, Vogl W, Koschelnik J, Epp M, Lackner M, Oismüller M, Kumpan M, Nemeth L, Strauss P, Sommer R, Ryzinska-Paier G, Farnleitner AH, Zessner M (2016) Real-time monitoring of beta-d-glucuronidase activity in sediment laden streams: A comparison of prototypes. *Water Res* 101:252–261. <https://doi.org/10.1016/j.watres.2016.05.072>
- Stange C, Thiem A (2020) Occurrence of antibiotic resistance genes and microbial source tracking markers in the water of a karst spring in Germany. *Sci Total Environ* 742. <https://doi.org/10.1016/j.scitotenv.2020.140529>
- Stevanovic Z (2019) Karst waters in potable water supply: a global scale overview. *Environ Earth Sci* 78(23):662. <https://doi.org/10.1007/s12665-019-8670-9>
- Veit H (2002) Die Alpen: Geoökologie und Landschaftsentwicklung (The Alps: geocology and landscape evolution), 1st edn. Eugen Ulmer Verlag, Stuttgart
- Wagner G (1950) Rund um Hochiften und Gottesackergebiet - Eine Einführung in das Werden und Vergehen einer Alpenlandschaft (Around Hochiften and Gottesacker area - an introduction to the growth and decay of an Alpine landscape). Verlag der Hohenloheschen Buchhandlung Ferdinand Rau, Öhringen
- White WB (1988) Geomorphology and hydrology of karst terrains. Oxford University Press, New York
- Wildeboer D, Amirat L, Price RG, Abuknesha RA (2010) Rapid detection of *Escherichia coli* in water using a hand-held fluorescence detector. *Water Res* 44:2621–2628. <https://doi.org/10.1016/j.watres.2010.01.020>
- World Health Organization (2017) Guidelines for drinking-water quality: fourth edition incorporating the first addendum. World Health Organization, Geneva. Licence: CC BY-NC-SA 3.0 IGO
- DIN 38402-62 (2014) German standard methods for the examination of water, waste water and sludge - General information (group A) - Part 62: Plausibility check of analytical data by performing an ion balance. Beuth Verlag GmbH, Berlin

Publisher's note Springer Nature remains neutral with regard to jurisdictional claims in published maps and institutional affiliations.